

Full Paper

Potentials of Nigella Sativa Oil as Inhibition towards the Corrosion of Mild Steel in Neutral Media

Abdelillah Benabida,¹ Mouhsine Galai,^{2,*} Mohamed Cherkaoui¹ and Omar Dagdag³

¹*Laboratory of materials, electrochemistry and environment, Faculty of Science, Ibn Tofail University, PB 133-14050 Kénitra, Morocco*

²*Laboratory of Materials Engineering and Environment: Modeling and Application, Faculty of Science, University Ibn Tofail BP. 133-14000, Kenitra, Morocco*

³*Laboratory of Polymers, Radiation and Environment- Team of Macromolecular & Organic Chemistry, Faculty of Science, University Ibn Tofail, BP 133, 14000 Kenitra, Morocco*

*Corresponding Author, Tel.: +212677235695

E-Mail: galaimouhsine@gmail.com

Received: 30 June 2016 / Received in revised form: 21 November 2016 /

Accepted: 26 November 2016 / Published online: 31 December 2016

Abstract- The application of Nigella sativa oil extract (NS) as a corrosion inhibitor for mild steel (MS) protection was investigated in neutral solution of 3% NaCl solution has been investigated by using weight loss method, potentiodynamic polarization and electrochemical impedance spectroscopy (EIS). Polarization curves indicate that NS is a cathodic inhibitor. The inhibition efficiency of NS reached 94% at 250 ppm. However, the adsorption of this inhibitor at the metallic surface is a physisorption type and follows the Langmuir isotherm adsorption. Thus the thermodynamic and kinetic parameters were calculated and discussed.

Keywords- Nigella sativa oil extract, Mild steel, Corrosion inhibition, EIS, Polarization

1. INTRODUCTION

Mild steel is widely used in most of the chemical industries for the fabrication of various reaction vessels, pipes, tanks, etc.; due to its easy availability and low cost, where they are deployed in various service environments containing alkalis and salt solutions are generally

used. The use of corrosion inhibitors is one of the most effective and economical methods to protect metal surfaces against corrosion in such aggressive media. A number of organic compounds have been reported as effective corrosion inhibitors, especially those containing nitrogen, oxygen, sulfur, phosphorus, and multiple bonds or aromatic rings in their structures. The lone pairs and π -electron distribution in these function groups are the key structural features that control the inhibition efficiency. Apart from the electronic structure considerations, there are also economic and toxicity considerations. Therefore, the focus now is to develop inexpensive, readily available and non-toxic (benign) corrosion inhibiting additives [1-4].

In this regard, immense number of scientific studies have been devoted to the inhibitive action of plant extracts on the corrosion of mild carbon steel in neutral solution, showing that these extracts could serve as good corrosion inhibitors; the cited extracts include; *Occimumviridis*, *Hibiscus*, *sabdariffa*, *Garciniakola*, *Phyllanthusamarus*, *Phaseolusvulgares* L [5-7].

The present study is aimed at investigating the inhibitive and adsorption properties of *Nigella sativa* oil (NS) on mild steel corrosion in 3% NaCl using gravimetric and electrochemical methods. NS is *Nigella* Seed (*Nigella sativa* L. 1753) or cumin black1 is an annual plant of the family Ranunculaceae native to Morocco and southwest Asia.

Usually, inhibition efficiency increases with the increase of inhibitor concentration until to achieve a steady state beyond some higher inhibitor concentration. However, some inhibitors may exhibit the peak-value-phenomenon of inhibitor concentration [8,9]. The concentration, where the peak-value-phenomenon (the lowest corrosion rate) is exhibited, is called the optimum concentration

The seeds are used as a traditional medicine or as a spice in many countries of the world (particularly in the Muslim world). Potentially toxic due to the presence of alkaloids and terpenoids; however they can be safely consumed in small quantities. The black cumin seeds have a high content of fatty oil (31%) consisting of glycerol ester of linoleic, oleic and palmitic. With further, phospholipids, glycolipids, tocopherols, sterols and that are especially active thymoquinone, the thymohydroquinone, and thymol and phenolics. The inhibition efficiency of this oil attains the maximum value of 94% at 250 ppm in neutral solution of NaCl 3%.

2. EXPERIMENTAL

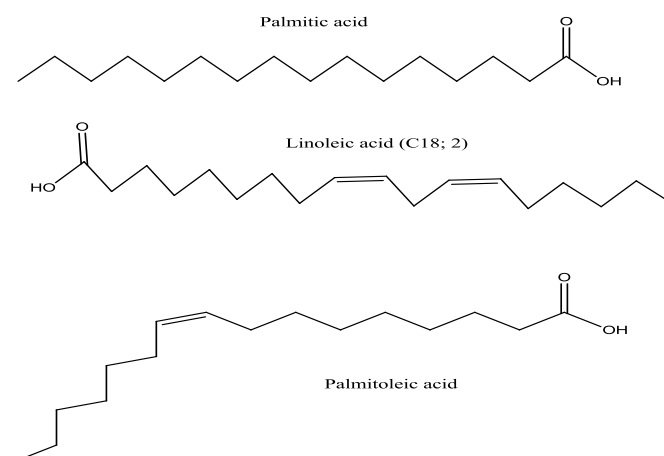
2.1. Inhibitor

Seeds of *Nigella sativa* L. (black cumin or black seeds) are widely used in traditional Islamic medicine and for culinary purposes worldwide. *Nigella* seed oil is becoming popular in and out of the Islamic world. Composition of *Nigella* seed oil is known to be location-

dependent. We investigated the composition of *Nigella* seed oil, prepared by solvent- or cold press-extraction of *Nigella* seeds grown in Morocco, Oil extraction yield was 37% and 27% when solvent or cold press extraction methods were used, respectively. In terms of oil major components, composition of *Nigella* seed oil from Morocco is similar to that from other Mediterranean countries known for their *Nigella* seed-oil quality. In *Nigella*, seed oil from Morocco, linoleic and oleic acids represented the main unsaturated fatty acids and accounted for more than 80% of the total fatty acids and the high linoleic/oleic acid ratio evidenced that such *Nigella* oil should not be used in fried food (Table 1). The oil fatty acid composition were identified by using gas chromatography method [10].

Table 1. Moroccan *Nigella* seed oil fatty acid composition (%)

Fatty acid	Cold press-extracted	Solvent-extracted
Myristic acid (C14:0)	1±0.1	0.2±0.1
Palmitic acid (C16:0)	13.1±0.2	11.9±0.2
Palmitoleic acid (C16:1)	0.2±0.1	0.2±0.1
Stearic acid (C18:0)	2.3±0.1	3.2±0.1
Octadecanoic acid (C18:1)	23.8±0.1	24.9±0.5
Linoleic acid (C18:2)	58.5±0.1	56.5±0.7
Linolenic acid (C18:3)	0.4±0.1	0.2±0.1
Arachidic acid (C20:0)	0.5±0.1	0.2±0.1
Saturated fatty acids	16.8±0.5	15.5±0.5
Unsaturated fatty acids	82.9±0.5	82.1±0.5



Scheme 1. Major constituent of *Nigella sativa* oil extract produced in Morocco

2.2. Corrosive medium

We used the neutral solution of 3% NaCl as a corrosive solution. We prepared 100 ml of 3% NaCl, namely 3 g of NaCl, which is dissolved in 100 ml of distilled water.

2.3. Specimens

Mild steel having the chemical composition C=0.5%, Mn=0.5%, S=0.05% and the remainder Fe was used for all experimental investigations. Rectangular specimens of the size 5 cm×1 cm×0.2 cm were used for weight loss measurements.

For polarization measurements, the working electrode was cut from mild steel with an exposed area of 1 cm². The samples were mechanically polished with different grades of emery papers, degreased with ethanol, washed with doubly distilled water and finally dried.

2.4. Weight loss measurements

Weight loss measurements were performed using 100 ml capacity beakers containing 100 ml test solution under total immersion in stagnant aerated condition at 298–328 K maintained in a thermostatic water bath. The pre-cleaned and weighed mild steel coupons were suspended in the beakers with the help of rods and hooks. The coupons were withdrawn at 2 h interval progressively for 10 h, cleaned as previously reported and reweighed. The weight loss, in grams, was taken as the difference in the weight of the mild steel coupons before and after immersion in different test solutions. Tests were performed for the blank solution (3% NaCl), solutions of 25-250 ppm ethanol and acetone extracts of coconut coir dust at different temperatures. The experiments were done in triplicate to ensure good reproducibility. The standard deviation values among parallel triplicate experiments were found to be smaller than 5%, indicating good reproducibility. From the weight loss values, corrosion rates were computed using the expression:

$$W = \frac{m_1 - m_2}{A \cdot t} \quad (1)$$

Where m_1 and m_2 are weight loss (mg) of mild steel coupons before and after immersion respectively in test solutions, A is the area of specimen (cm²) and t is the exposure time (h). The inhibition efficiency ($E\%$) was computed using Eq. (2):

$$E\% = \frac{\omega_{blank} - \omega_{inh}}{\omega_{blank}} \quad (2)$$

Where ω_{blank} and ω_{inh} are the corrosion rate in the absence and presence of the inhibitor respectively in 3% NaCl at the same temperature.

2.5. Electrochemical measurements

The electrochemical measurements were carried out using Volta lab (Tacussel-Radiometer PGZ 100) potentiostat and controlled by Tacussel corrosion analysis software model (Voltmaster 4) at under static condition. The corrosion cell used had three electrodes. The reference electrode was a (Ag/AgCl) (3 M KCl). A platinum electrode was used as auxiliary electrode of surface area of 1 cm². The working electrode was mild steel. All potentials given in this study were referred to this reference electrode. The working electrode was immersed in test solution for 30 min to a establish steady state open circuit potential (E_{ocp}). After measuring the E_{ocp} , the electrochemical measurements were performed. All electrochemical tests have been performed in aerated solutions at 298 K. The EIS experiments were conducted in the frequency range with high limit of 100 kHz and different low limit 0.1 Hz at open circuit potential, with 10 points per decade, at the rest potential, after 30 min of acid immersion, by applying 10 mV ac voltage peak-to-peak. Nyquist plots were made from these experiments.

After ac impedance test, the potentiodynamic polarization measurements of mild steel substrate in inhibited and uninhibited solution were scanned from cathodic to the anodic direction, $E = E_{corr} \pm 200$ mV, with a scan rate of 1 mV s⁻¹. The potentiodynamic data were analysed using the polarization VoltaMaster 4 software. The linear Tafel segments of anodic and cathodic curves were extrapolated to corrosion potential to obtain corrosion current densities (I_{corr}). From the polarization curves obtained, the corrosion current (I_{corr}) was calculated by curve fitting using the equation 3:

$$I = I_{corr} \left[\exp\left(\frac{2.3\Delta E}{\beta_a}\right) - \exp\left(\frac{2.3\Delta E}{\beta_c}\right) \right] \quad (3)$$

The inhibition efficiency was evaluated from the measured I_{corr} values using the following relationship:

$$\eta_{Tafel} (\%) = \frac{I_{corr} - I_{corr(i)}}{I_{corr}} \times 100 \quad (4)$$

Where I_{corr} and $I_{corr(i)}$ are the corrosion current densities for steel electrode in the uninhibited and inhibited solutions, respectively.

3. RESULTS AND DISCUSSION

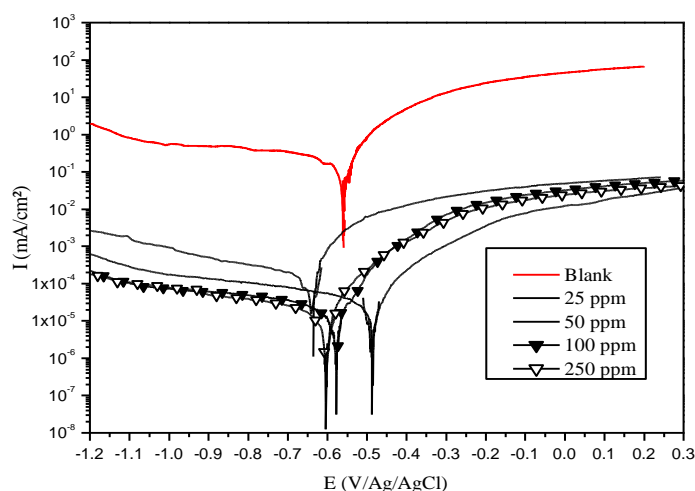
3.1. Gravimetric measurements

Values of the inhibition efficiency and corrosion rate obtained from the weight loss measurements of mild steel for different concentrations of NS in 3% NaCl at 298 K after 24 h of immersion are given in table 2.

Table 2. Corrosion rate of carbon steel and inhibition efficiency at different concentrations of NS in 3% NaCl obtained from weight loss and surface coverage (θ) measurements at 298 K

	Concentration [©] (ppm)	W_{corr} ($\text{mg}/\text{cm}^2\text{h}^1$)	$E\%$	θ
Blank	00	0.3	-	-
NS	25	0.042	86	0.84
	50	0.047	84	0.86
	100	0.029	90	0.90
	250	0.028	91	0.91

It can be seen from table 2 that results indicate that the compound NS in question inhibit mild steel corrosion in 3% NaCl, the efficiency values of inhibition increases substantially with the increase of the concentration of the inhibitor, , and reaches a maximum value of 91% at 250 ppm of NS.

**Fig. 1.** Polarization curves for mild steel in 3% NaCl in the absence and presence of various concentrations of NS after 30 mn of immersion at 298 K

This behavior could be attributed due to interaction of compounds with the metal surface that results in the adsorption of inhibitor molecules[11]. The lone pair of electron on the oxygen will co-ordinate with the metal atoms of active sites. The presence of higher electron density on acid group as well as π -electrons in NS causes stronger interaction with metal surface [12].

3.2. Polarization measurements

The anodic and cathodic polarization behavior of mild steel in the presence and absence of NS in 3% NaCl is shown in Fig. 1. Various corrosion parameters such as corrosion current density (I_{corr}), corrosion potential (E_{corr}), Tafel slopes (β_c and β_a) and inhibition efficiencies ($\% \eta$) are given in Table 3.

From the results obtained, we note on the one hand, a decrease of current densities on the two cathodic and anodic branches after the addition of different concentrations of NS with increasing inhibitory efficiency and an achieved concentration of a maximum value of 94% at 250 ppm.

Table 3. Summarizes the different electrochemical parameters associated with mild steel polarization curves in 3% NaCl at different concentrations NS

	<i>C</i> (ppm)	<i>E_{corr}</i> (mV/Ag/AgCl)	<i>I_{corr}</i> ×10 ⁶ (A/cm ²)	<i>β_c</i> (mV)	<i>β_a</i> (mV)	<i>η</i> %
Blank	00	-559	280	121	121	-
	25	-419	151	538	142	46
	50	-469	31	151	547	90
NS	100	-562	19	557	14.7	93
	250	-579	15	525	122	94

3.3. Electrochemical impedance spectroscopy

To confirm the results obtained by the polarization curves and to extract more information about the corrosion mechanisms, we used some techniques of electrochemical impedance. The Nyquist diagrams obtained in 3% NaCl medium in the absence and presence of different concentrations for NS after one 30 mn of immersion at 298 K are shown respectively in Figure 2.

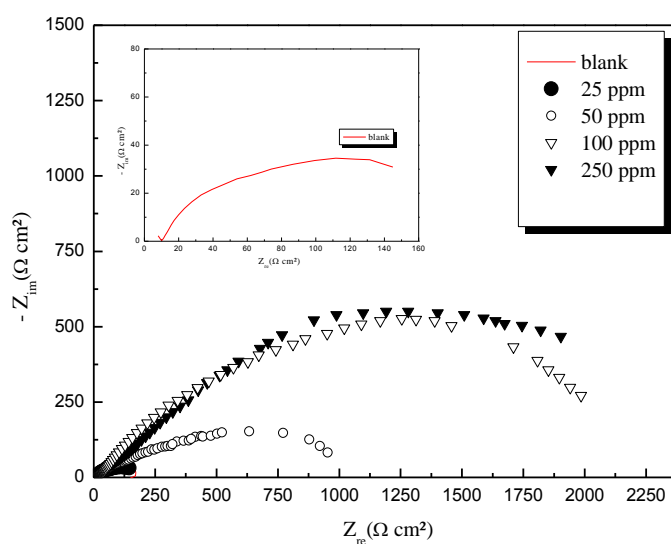


Fig. 2. Nyquist diagrams for mild steel electrode with and without NS at different concentrations after 30 mn of immersion

We notice that the diameter of the half-circles, relative to the witness, increases with increasing concentrations of inhibitor, which means that increasing concentrations lead to an increase of the inhibiting effect, hence a delay of iron dissolution speed due to the formation of a protective film on the surface of the electrode [13].

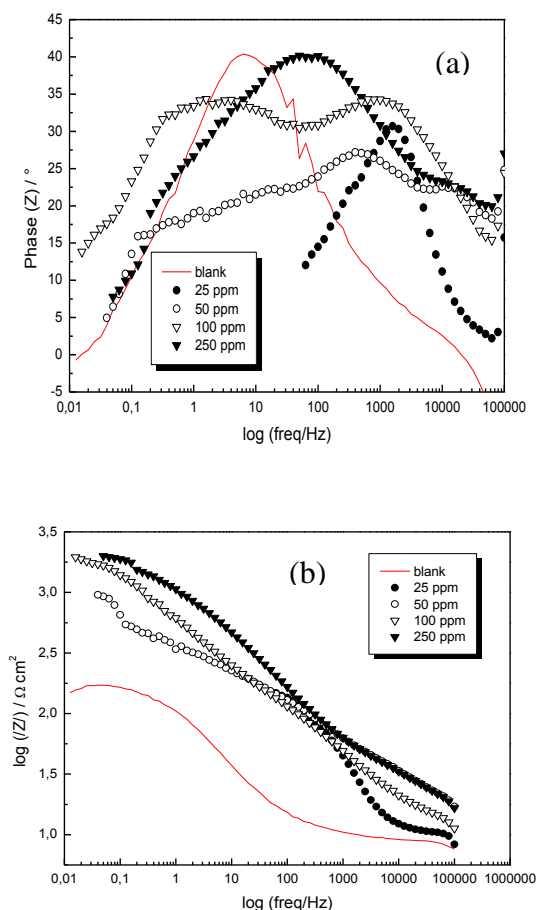


Fig. 3. (a) and (b) the Bode plots for carbon steel in 3% NaCl at different concentrations of NS

Table 4. Electrochemical impedance parameters for corrosion of mild steel in 3% NaCl at various contents of NS

	C (M)	R_s ($\Omega \cdot \text{cm}^2$)	R_f ($\Omega \cdot \text{cm}^2$)	C_f ($\mu\text{F}/\text{cm}^2$)	C_{dl} ($\mu\text{F}/\text{cm}^2$)	R_{ct} ($\Omega \cdot \text{cm}^2$)	R_p ($\Omega \cdot \text{cm}^2$)	$\eta\%$
Blank	00	10	175	201	-	-	165	-
NS	25	16	31	68	116	289	304	46.00
	50	42	308	12	37	992	1258	86.60
	100	10	459	5.5	19	1948	2397	93.11
	250	09	234	3	3	2311	2536	93.50

The impedance data of carbon steel recorded after 30 min of electrode immersion 3% NaCl with and without NS are presented as Bode plots in Fig. 3. The Bode plots show two phase maxima at intermediate and low frequencies.

The examination of Table 4 show that C_{dl} and C_f values decrease while the values of R_{ct} increase when the concentration of NS increases. The significant decrease in capacitance values can be attributed to a decrease in the dielectric constant or increasing the thickness of the electrical double layer due to the adsorption of the inhibitor forming a protective layer on the mild steel surface [14].

Similarly, when the concentration of inhibitor increases, the values of charge transfer resistance R_{ct} increase. These respective evolutions of R_{ct} suggests that the amount of inhibiting molecules formed on carbon steel increases, and consequently the decrease of active sites becomes necessary for the reactions of iron dissolution.

The equivalent circuit model employed for these systems is presented in Figure 4.

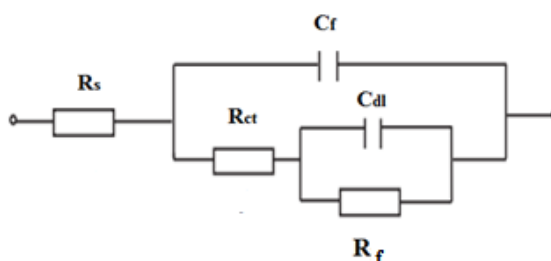


Fig. 4. The electrochemical equivalent circuit used to fit the impedance spectra. Where: **R_s** is solution resistance, **R_{ct}** is charge transfer resistance, **R_f** is the film resistance, **C_f** is the film capacitance, and **C_{dl}** is the double layer capacitance.

3.4. Adsorption isotherm and thermodynamic consideration

The adsorption of organic inhibitors on metal surface can markedly change the corrosion resisting properties of the metals. Therefore, the investigation of relation between the adsorption and corrosion inhibition is important [15].

The adsorption isotherms can give valuable information on the interaction of inhibitor and metal surface. So, it is essential to know the mode of adsorption and the adsorption isotherm. Several adsorption isotherms were assessed and the Langmuir adsorption isotherm was found to be the best description of the adsorption behaviour of the studied inhibitor, which obeys the following Eqs. (5) and (6)[16]:

$$\frac{\theta}{1-\theta} = K_{ads} C_{inh} \quad (5)$$

$$K_{ads} = \frac{1}{55.55} \exp \left(-\frac{\Delta G_{ads}^{\circ}}{RT} \right) \quad (6)$$

C_{inh} is the inhibitor concentration, θ is the fraction of the surface coverage, K_{ads} is the adsorption equilibrium constant and ΔG_{ads}° is the standard free energy of adsorption.

Figure 5 shows the dependence of the fraction of the surface coverage C_{inh}/θ as a function of the concentration (C_{inh}) of NS.

The degree of surface coverage θ for different concentrations of the inhibitor in 3% NaCl has been evaluated from polarization curve measurements. The obtained plot of C_{inh}/θ vs C_{inh} is linear and it is presented in figure 5. The regression coefficient is $R^2=0.999$. The intercept permits the calculation of the adsorption equilibrium constant K_{ads} which is equal 34.4867 M^{-1} and leads to evaluate $\Delta G_{ads}^{\circ}=-18.71 \text{ kJ mol}^{-1}$. The value of ΔG_{ads}° indicates the low interaction between inhibitor molecules and the steel surface [17,18].

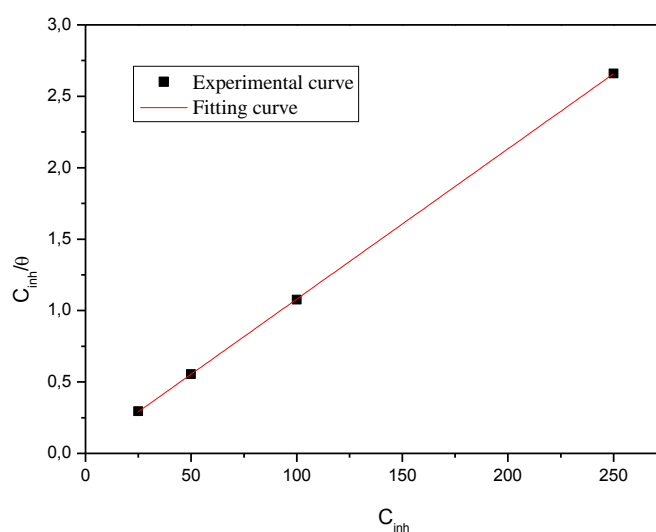


Fig. 5. Langmuir adsorption plot of mild steel in 3% NaCl solution containing various concentrations of NS

3.5. Effect of temperature

The effect of temperature on the inhibited metal/3% NaCl reaction is complex, because many changes occur on the metal surface such as rapid etching and desorption of inhibitor and the inhibitor itself may undergo decomposition. The change of the corrosion rate with the temperature was studied in 3% NaCl, both in absence and presence of NS. For this purpose, polarization readings were performed at different temperatures from 298 to 328 K in absence and presence of 250 ppm of NS (Fig. 6). The electrochemical parameters were extracted and summarized in Table 5. Corrosion inhibition efficiencies (η %) calculated from Eq. 4 are also shown in Table 5. Fig. 5 shows that raising the temperature shifts corrosion potentials to nobler potentials. As seen, this led to a higher corrosion rate (I_{corr}).

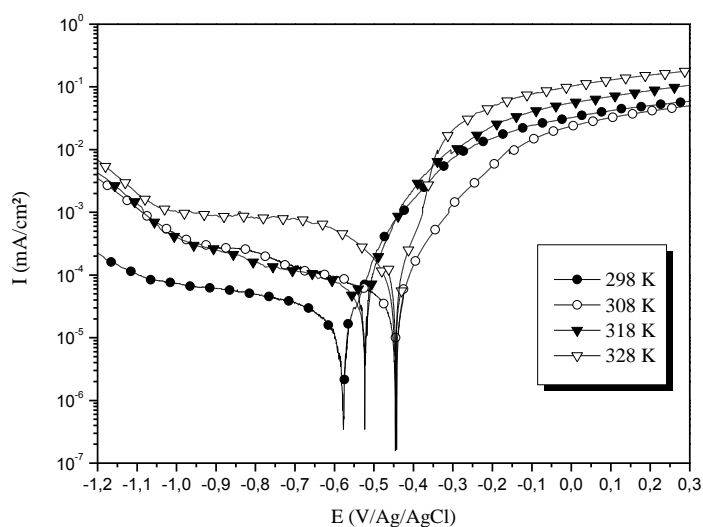


Fig. 6. Potentiodynamic polarisation curves of mild steel in 3% NaCl in the presence of 250 ppm of NS at different temperatures

Table 5. Electrochemical parameters and the corresponding inhibition efficiencies at various temperature studied of mild steel in 3% NaCl in absence and presence 250 ppm of NS

T (K)	E_{corr} mV/Ag/AgCl		$I_{corr} \times 10^6$ (A/cm ²)		η %
	Blank	250 ppm of NS	Blank	250 ppm of NS	
298	-559	-579	280	15	94
308	-568	-427	345	39	88
318	-653	-508	556	68	87
328	-677	-422	706	131	81

An inspection of Table 5 shown that, as the temperature increased, the values of I_{corr} increase and η (%) decrease. This behaviour reflects physical adsorption of NS on the steel surface [19].

3.6. Kinetic parameters of activation corrosion process

Effect of temperature on the corrosion parameter can be deduced by comparing the activation energy in the presence and absence of the inhibitor. In order to calculate the activation energy of the corrosion process and investigation of the mechanism of inhibition, polarization measurements was carried out at various temperatures. The dependence of the corrosion rate on temperature can be expressed by the Arrhenius equation (7) [20-23]:

$$i_{corr} = A \exp \left(-\frac{E_a}{RT} \right) \quad (7)$$

Where i_{corr} is corrosion current, A is the constant, E_a is the activation energy of the metal dissolution reaction, R is the gas constant and T is the temperature. Arrhenius plots for the corrosion rate of carbon steel were given in Figure 7.

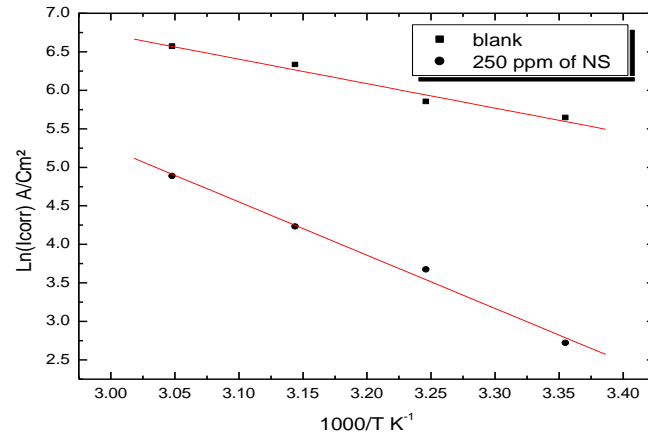


Fig. 7. The relationship between Ln (i_{corr}) and $1/T$ for mild steel in 3% NaCl in the absence and presence of NS

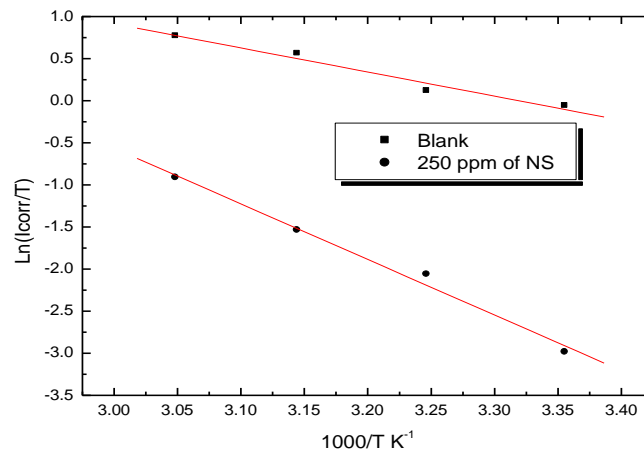


Fig. 8. Transition state plots for mild steel in 3% NaCl in the absence and presence of 250 ppm concentration of NS

Value of E_a for mild steel in 3% NaCl and presence of the optimum concentration 250 ppm of the inhibitor were estimated by calculating the slope of Ln (i_{corr}) vs. $1/T$. Moreover, the Arrhenius equation can be converted an alternative Eq 8 as follow[24]:

$$i_{corr} = \frac{RT}{hN} \exp\left(\frac{\Delta S_a}{R}\right) \exp\left(-\frac{\Delta H_a}{RT}\right) \quad (8)$$

Where N is Avogadro's constant, h is the Plank's constant, ΔS_a is the entropy of activation and ΔH_a is the enthalpy of activation (Figure 8). A plot of $\ln(i_{\text{corr}}/T)$ against $1/T$ should give a straight line with a slope of $(\Delta H_a/T)$ and intercept of $[\ln(R/Nh) + (\Delta S_a/R)]$, E_a , ΔH_a and ΔS_a were calculated and tabulated in Table 6.

Table 6. The influence of temperature on the electrochemical parameters for mild steel in 3% NaCl and 250 ppm of NS

	E_a (kJ/mol)	ΔH_a (kJ/mol)	ΔS_a (J.mol ⁻¹ K ⁻¹)
Blank	26.3	24	-120
250 ppm of NS	57.42	54.8	-37.6

The important fact is that the activation energy for the corrosion of carbon steel in that solution has been increased from 26.3 to 57.48 kJ/mol by adding the NS corrosion inhibitor, which indicates that required energy for carbon steel corrosion has been increased by adding the inhibitor i.e. corrosion current has been increased by addition of NS corrosion inhibitor. The increase in the apparent activation energy may be interpreted as physical adsorption that occurs in the first stage [25]. It is well known that decrease in efficiency with the increase of temperature is attributed to the physical adsorption [26]. The results show that the addition of NS decreases metal dissolution in 3% NaCl medium. This hindrance to dissolution is due to the formation of the metal complex layer [27]. Large and negative values of entropies show that the activated complex in the rate determining step represents an association rather than a dissociation step, meaning that a decrease in disordering takes place on going from reactants to the activated complex [28,29]. The values of ΔS_a in the presence of NS are large and negative that is accompanied with exothermic adsorption process [30].

4. CONCLUSION

The inhibition efficiency of mild steel corrosion in 3% NaCl by NS has been investigated by using weight loss test and electrochemical measurement. The following conclusions were drawn from this study:

- Reasonably good agreement was observed between potentiodynamic polarization and electrochemical impedance spectroscopy techniques.
- The examined NS shows excellent inhibition properties for the corrosion of mild steel in 3% NaCl at 298 K, the efficiency values of inhibition increases with increasing the

concentration of the inhibitor. The maximum inhibition efficiency of 94% was observed at 250 ppm concentration.

- The effectiveness of inhibition NS slowly decreases with temperature.
- The adsorption of NS on the mild steel surface from 3% NaCl obeys a Langmuir adsorption isotherm.

REFERENCES

- [1] R. M. K. Ramya, K. K. Anupama, and A. Joseph, *Mater. Chem. Phys.* 149-150 (2015) 632.
- [2] P. E. A. María, V. Fiori-Bimbi, H. Vaca, C. A. Gervasi, *Corrosion Science* 92 (2015) 192.
- [3] P. S. P. PreethiKumari, Suma A. Rao, *Int. J. Corros.* (2014) 1.
- [4] M. A. J. Mazumder, H. A. Al-Muallem, and S. A. Ali. *Corros. Sci.* 90 (2015) 54.
- [5] E. E. Oguzie, *Corros. Sci.* 50 (2008) 2993.
- [6] P. C. Okafor, M. E. Ikpi, I. E. Uwaha, E. E. Ebenso, U. J. Ekpe, and S. A. Umoren, *Corros. Sci.* 50 (2008) 2310.
- [7] A. M. Abdel-Gaber, B. A. Abd-El-Nabey, I. M. Sidahmed, A. M. El-Zayady, and M. Saadawy, *Corros. Sci.* (2006) 2765.
- [8] I. Singh, *Corros. Sci.* 49 (1993) 473.
- [9] J. Wang, Ph.D. Dissertation, Institute of Corrosion and Protection of Metals, Chinese Academy of Sciences (1990).
- [10] S. Gharby, H. Harhar, D. Guillaume, A. Roudani, S. Boulbaroud, M. Ibrahimi, M. Ahmad, S. Sultana, T. B. Hadda, and I. Chafchaoui-Moussaoui, *J. Saudi Soc. Agricultural Sci.* 14 (2015) 172.
- [11] O. Dagdag, M. Galai, M. Ebn Touhami, A. Essamri, and A. Elharfi, *Der Pharm. Chem.* 7 (2015) 284.
- [12] O. Dagdag, M. Galai, R. Ziraoui, M. Ebn Touhami, A. Essamri, and A. El Harfi, *Der Pharm. Chem.* 7 (2015) 46.
- [13] X. Zhou, H. Yang, and F. Wang, *Corros. Sci.* 54 (2012) 193.
- [14] A. Popova, E. Sokolova, S. Raicheva, and M. Christov, *Corros. Sci.* 45 (2003) 33.
- [15] B. H. S. Kertit, *Appl. Surf. Sci.* 93 (1996) 59.
- [16] K. F. Khaled, *Mater. Chem. Phys.* 112 (2008) 104.
- [17] B. J. O.M. Drazic, *Electrochim. Acta* 7 (1962) 293.
- [18] V. Branzoi, M. Branzoi, and F. Baibarac, *Mater. Chem. Phys.* 65 (2000) 288.
- [19] M. C. A Popova, and A. Vasilev, *Corros. Sci.* 49 (2007) 3276.
- [20] E. Oguzie, C. K. Enenebeaku, C. E. Ogukwe, M. A. Chidiebere, and K. L. Oguzie, *J. Phys. Chem. C* 116 (2012) 13603.

- [21] A. D. N. Dkhireche, A. Rochdi, J. Hmimou, R. Tourir, M. E. Touhami, M. El Bakri, A. El Hallaoui, A. Anouar, and H. Takenouti, *J. Ind. Eng. Chem.* 19 (2013) 1996.
- [22] S. D. X. Li, and H. Fu, *Corros. Sci.* 53 (2011) 664.
- [23] S. D. X. Li, and H. Fu, *Corros. Sci.* 55 (2012) 280.
- [24] A. Y. Musa, A. Bakar Mohamad, A. A. H. Kadhum, M. S. Takriff, L. T. Tien, *Corros. Sci.* 53 (2011) 3672.
- [25] S. Martinez, and I. Stern, *Appl. Surf. Sci.* 199 (2002) 83.
- [26] A. A. Khadom, *J. Chilean Chem. Soc.* 59 (2014) 2545.
- [27] L. R. Chauhan, and G. Gunasekaran, *Corros. Sci.* 49 (2007) 1143.
- [28] I. S. S. Martinez, *Appl. Surf. Sci.* 199 (2002) 83.
- [29] J. Marsh, *Advanced Organic Chemistry*, third ed., Wiley Eastern, New Delhi (1988).
- [30] E. A. Noor, *Int. J. Electrochem. Sci.* 2 (2007) 996.